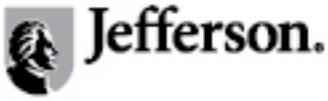



3-21-2014

# Isoform- and species-specific control of inositol 1,4,5-trisphosphate (IP3) receptors by reactive oxygen species.

Száva Bánsághi
*Thomas Jefferson University*, szava.bansaghi@jefferson.edu

Tünde Golenár
*Thomas Jefferson University*, tunde.golenar@jefferson.edu

Muniswamy Madesh
*Thomas Jefferson University*, Muniswamy.madesh@jefferson.edu

György Csordás
*Thomas Jefferson University*, Gyorgy.Csordas@jefferson.edu

Satish P. RamachandraRao
*Thomas Jefferson University*, Satish.Rao@jefferson.edu

***See next page for additional authors***

**Authors**
Száva Bánsághi, Tünde Golenár, Muniswamy Madesh, György Csordás, Satish P. RamachandraRao, Kumar Sharma, David I Yule, Suresh K Joseph, and György Hajnóczky

# Isoform-and species-specific control of $IP_3$ receptors by reactive oxygen species*

Száva Bánsághi[1], Tünde Golenár[1], Muniswamy Madesh[1], György Csordás[1], Satish RamachandraRao[2], Kumar Sharma[2], David I.Yule[3], Suresh K. Joseph[1] and György Hajnóczky[1]

[1]MitoCare Center, Department of Pathology, Anatomy and Cell Biology, Thomas Jefferson University, Philadelphia, PA 19107,
[2]Center for Novel Therapies for Kidney Disease, Department of Medicine, Thomas Jefferson University, Philadelphia, PA 19107,
[3]Department of Pharmacology and Physiology, University of Rochester Medical Center, Rochester, NY 14642.

SB, TG and MM contributed equally to this paper.

*Running title: Control of $IP_3$ receptors by reactive oxygen species

To whom correspondence should be addressed: Dr. György Hajnóczky, MitoCare Center Suite 527 JAH Thomas Jefferson University Philadelphia PA 19107 USA
Tel. (215) 503-1427 Fax. (215) 923-2218 E-mail. gyorgy.hajnoczky@jefferson.edu

Keywords: calcium signaling, $IP_3$ receptor, reactive oxygen species, ROS, endoplasmic reticulum, mitochondria

**Background:** Reactive oxygen species (ROS) affect cytoplasmic calcium signaling.
**Results:** Superoxide anion causes oxidation of the $IP_3$ receptor and sensitization of calcium release to promote cytoplasmic calcium oscillations and mitochondrial calcium uptake.
**Conclusion:** Physiologically relevant ROS controls cytoplasmic and mitochondrial calcium transport through $IP_3$ receptors.
**Significance:** Mechanisms of calcium and ROS interactions are relevant for both physiological and pathophysiological signaling.

**Abstract:**
Reactive oxygen species (ROS) stimulate cytoplasmic $[Ca^{2+}]$ ($[Ca^{2+}]_c$) signaling but the exact role of the $IP_3$ receptors (IP3R) in this process remains unclear. IP3Rs serve as a potential target of ROS produced by both ER and mitochondrial enzymes, which might locally expose IP3Rs at the ER-mitochondrial associations. Also, IP3Rs contain multiple reactive thiols, common molecular targets of ROS. Therefore, we have examined the effect of superoxide anion ($O_2^{\cdot-}$) on IP3R-mediated $Ca^{2+}$ signaling. In human HepG2, rat RBL-2H3, and chicken DT40 cells, we observed $[Ca^{2+}]_c$ spikes and frequency-modulated oscillations evoked by a $O_2^{\cdot-}$ donor, xanthine (X)+xanthine oxidase (XO), dose-dependently. The $[Ca^{2+}]_c$ signal was mediated by ER $Ca^{2+}$ mobilization. X+XO added to permeabilized cells promoted the $[Ca^{2+}]_c$ rise evoked by submaximal doses of $IP_3$, indicating that $O_2^{\cdot-}$ directly sensitizes IP3R-mediated $Ca^{2+}$ release. In response to X+XO, DT40 cells lacking two out of three IP3R isoforms (DKO) expressing either type 1 (DKO1) or type 2 IP3Rs (DKO2) showed a $[Ca^{2+}]_c$ signal, whereas DKO expressing type 3 IP3R (DKO3) did not. By contrast, IgM that stimulates $IP_3$ formation, elicited a $[Ca^{2+}]_c$ signal in every DKO. X+XO also facilitated the $Ca^{2+}$ release evoked by submaximal $IP_3$ in permeabilized DKO1 and DKO2 but was ineffective in DKO3 or in DT40 lacking every IP3R (TKO). However, X+XO could also facilitate the effect of suboptimal $IP_3$ in TKO transfected with rat IP3R3. Although, in silico studies failed to identify a thiol missing in the chicken IP3R3, an X+XO-induced redox change was documented only in the rat IP3R3. Thus, ROS seem to specifically sensitize IP3Rs through a thiol group(s) within the IP3R, which is probably unaccessible in the chicken IP3R3.

## Introduction

Inositol 1,4,5-trisphosphate receptors (IP3R) are $Ca^{2+}$ channels that serve to release $Ca^{2+}$ from the endoplasmic reticulum (ER) in response to cell stimulation by a wide array of hormones, growth factors and neurotransmitters (1,2). Many fundamental biological processes that are activated or regulated by $Ca^{2+}$ signals require IP3R function. These include such critical functions as secretion (3), smooth muscle contraction (4), gene transcription (5) and fertilization (6). $Ca^{2+}$ release from IP3Rs localized in the vicinity of mitochondria also plays a pivotal role in propagation of $Ca^{2+}$ signals into the mitochondrial matrix which, depending on the exact conditions, can lead to enhanced ATP synthesis or the initiation of apoptotic signaling (7). $IP_3R$ channel activity is primarily regulated by $IP_3$ and $Ca^{2+}$ concentrations although the channel is also modulated by phosphorylation (8), ATP (9) and interaction with a large number of proteins (10).

Another factor that regulates IP3Rs is the cellular redox state although the molecular basis for this mode of regulation is poorly understood (reviewed in (11)). Various exogenously added oxidants stimulate IP3R-mediated $Ca^{2+}$ release. This includes thimerosal (12-14), t-butylhydroperoxide (15) and diamide (16,17). In the case of thimerosal the proposed mechanism involves an increased sensitivity of the receptor to lower [$IP_3$] which in some cells is sufficient to trigger $Ca^{2+}$ oscillations at the ambient [$IP_3$] present in unstimulated cells (11). While sensitization to $IP_3$ may be a general mechanism applicable to other oxidants, it has also been suggested that they may alter the $Ca^{2+}$ sensitivity of the receptor (15,16).

Three different IP3R isoforms are expressed in different amounts in various cells and the different isoforms are capable of forming homo and heterotetramers (18,19). The selective localization or regulation of individual isoforms have been proposed to play a role in different biological processes. For example the IP3R3 isoform has been suggested to have the predominant role in supplying $Ca^{2+}$ to the mitochondria in CHO cells (20). However, little is known regarding the IP3R isoform selectivity for regulation by redox agents. IP3Rs located at ER/mitochondrial junctions would be particularly prone to the reactive oxygen species (ROS) derived from both organelles. In contrast to the exogenous reagents added to manipulate the cellular redox state, the primary endogenous ROS generated as a consequence of mitochondrial respiratory chain activity are superoxide anions ($O_2^-$) which are dismutated to form $H_2O_2$. Similarly, the ER can generate substantial amounts of $H_2O_2$ from multiple sources (21). In the present study we have evaluated the effects on IP3R-mediated release of a physiological oxidant, $O_2^-$ generated from xanthine by xanthine oxidase. The experiments have been carried out using different experimental models which express individual isoforms of IP3Rs. Our data show that responsiveness to an endogenously produced ROS is dependent on the exact IP3R isoform and species variant examined.

## Experimental Procedures

**Cells**: RBL-2H3, HepG2 and DT40 (wildtype and IP3R knockouts alike) cells were cultured as described previously (7,22,23). Stable colonies of DT40 IP3R triple knockout cells rescued by rat IP3R3 were produced as described previously (24). Expression of the IP3R3 in each clone was assessed by western blotting.

**Measuring changes in the redox state of $IP_3Rs$**: The method employed was modified from the "thiol trapping" procedure described by (25) in which TCA is used to preserve the thiol redox state of the proteins. DT40 cells expressing the endogenous chicken IP3R3 or the rat IP3R3 were centrifuged (800 g, 5 min) and resuspended in an extracellular like medium containing 0.25 % BSA (0.25 % BSA-ECM). Aliquots 2.5 ml (~2 x $10^7$ cells/ml) were treated for 5 min with 0.1 mM Xanthine and 20 mU/ml Xanthine oxidase. The samples were rapidly centrifuged (1,500 g, 1min), resuspended in 0.5 ml PBS and quenched by addition of TCA to a final concentration of 10% (w/v). The TCA pellet was recovered by centrifugation (3,000 g, 5min) and dissolved in denaturing buffer (DB) containing 6 M Urea, 0.5 % SDS, 200 mM TrisHCl (pH 8.0) and 10mM EDTA. Free thiol groups in the lysate were blocked by reaction with 10 mM iodoacetamide for 30 min followed by re-precipitation with TCA and solubilization in DB buffer. Modified thiol groups on the receptor were converted to the reduced form by reaction with 10 mM DTT for 30min. The lysate was again reprecipitated with

TCA and re-solubilized in DB buffer containing 20 μM DTT at a protein concentration of 2-3 mg/ml. Free thiol groups present in the receptor from control and X+XO treated cells were reacted in a final volume of 25 μl with 0.5 mM PEG-maleimide (5 kDa, Fluka). Gel shifts in the IP3R were visualized after running the samples on 5 % SDS PAGE mini-gels and immunoblotting with a monoclonal Ab to the IP3R3 isoform (BD Biosciences).

**Fluorescence imaging of $[Ca^{2+}]$ in single cells:** To monitor $[Ca^{2+}]_c$, cells were loaded with 5 μM fura2/AM for 20 min in the presence of 100 μM sulfinpyrazone and 0.003% (wt/v) pluronic acid in 2 % BSA-ECM at room temperature. Cells attached to coverslips were placed in 1 ml buffer to the heated stage (35 Cº) of an inverted epifluorescence microscope (40X oil objective) connected to a cooled CCD camera (PXL, Photometrics). Ratiometric imaging of fura2 was used to monitor $[Ca^{2+}]$ as described previously (7,26,27). Simultaneous imaging of cytoplasmic $[Ca^{2+}]$ and GSH/GSSG was performed in cells transfected with plasmid DNA encoding RCaMP (28) and Grx1-roGFP2 (29,30) using a ProEM1024 EM-CCD (Princeton Instruments), fitted to Leica DMI 6000B inverted epifluorescence microscope (31). Two different filter sets (for RCaMP: ex:580/20 nm, bs595 nm, em: 630/60 nm and for Grx1-roGFP2: ex: 415/20 nm and 490/20 nm excitation filters and a 500 nm long-pass bs and ex:520/40nm) were alternated by a motorized turret.

**Fluorometric measurements of $[Ca^{2+}]_c$ and $[Ca^{2+}]_m$ in suspensions of permeabilized cells**: Experiments with the RBL-2H3 cells were carried out as described earlier (26). Before recording, the fura2FF/AM-loaded cells (approx. 2 mg protein/1.5 ml) were permeabilized in an intracellular medium (ICM: KCl 120 mM, NaCl 10 mM, $KH_2PO_4$ 1 mM, Tris-HEPES 20 mM, MgATP 2 mM, and antipain, leupeptin and pepstatin 1 μg/ml each at pH 7.2) supplemented with 25 μg/ml digitonin for 5 min at 35˚C, followed by washout of the released cytosolic fura2FF (125 g for 4-5 min). Compartmentalized fura2FF has been shown to occur in the mitochondria of the RBL-2H3 cells (22). Permeabilized cells were resuspended in ICM supplemented with succinate 2 mM and rhod2/FA 0.25 μM and maintained in a stirred thermostated cuvette at 35˚C. Rhod2/FA was added to monitor $[Ca^{2+}]$ in the intracellular medium that exchanges readily with the cytosolic space and so $[Ca^{2+}]_{rhod2}$ was abbreviated as $[Ca^{2+}]_c$.

When $[Ca^{2+}]_c$ was measured in permeabilized DT40 cells, the harvested cells were first preincubated in $Ca^{2+}$-free extracellular buffer for 1hr at 37°C to drain $Ca^{2+}$ from intracellular compartments and stored on ice. Cells were permeabilized with saponin (40 μg/ml) and incubated in ICM and to measure $[Ca^{2+}]_c$ fura2/FA 1.5 μM was added.

Fluorescence was monitored in a fluorometer (Delta-RAM, PTI) using 340 nm, 380 nm excitation and 500 nm emission for fura2 or fura2FF and 540 nm excitation and 580 nm emission for rhod2. Calibration of the fura2, fura2FF and rhod2 fluorescence was carried out at the end of each measurement as described previously (26).

**Statistics:** Experiments were carried out with at least 3 different cell preparations and the data are shown as mean±SE. Significance of differences from the relevant controls was calculated by Student's *t* test.

## Results

### $O_2^{\cdot-}$-induced frequency-modulated $[Ca^{2+}]_c$ oscillations in HepG2 cells

Addition of a $O_2^{\cdot-}$-generating system (32) to HepG2 human hepatocarcinoma cells resulted in a $[Ca^{2+}]_c$ spike in most cells within 1 min (Fig1A). The initial spike was followed by $[Ca^{2+}]_c$ oscillations (Fig1A). Typically, $[Ca^{2+}]_c$ returned close to the basal level among the individual spikes, giving rise to a baseline-spike pattern (Fig1A,B). The lagtime and the fraction of the responsive cells were inversely and directly proportional to the amount of the $O_2^{\cdot-}$-generating enzyme, respectively (Fig1BCD). The mean response of the cells on the field also showed an initial $[Ca^{2+}]_c$ rise and a subsequent decay to a plateau level (Fig1B lower). The height of both the spike and the plateau was proportional with the added amount of the $O_2^{\cdot-}$-generating enzyme (Fig1BE). The $[Ca^{2+}]_c$ signal was prevented by heat inactivation of the $O_2^{\cdot-}$-generating enzyme (Fig1E) or when the $O_2^{\cdot-}$-generating system was applied to cells pretreated with a cell permeable SOD mimetic, MnTBAP (20 μM**,** not shown).

Previous studies have demonstrated that addition of the $O_2^{\cdot-}$-generating system to intact cells results in a rapid increase in intracellular $O_2^{\cdot-}$ using both roGFP2 (33) and MitoSox (34). Here, we recorded the cytoplasmic glutathione redox state simultaneously with $[Ca^{2+}]_c$. Although glutathione redox might change with a slower kinetic than superoxide anion, it can be measured in a more specific and reliable manner. These measurements showed a change in the redox starting together with the X+XO-induced first $[Ca^{2+}]_c$ spike ($p<0.03$ at 1min) (Fig2). Since the signal to noise ratio is much lower for the redox sensors than that for the calcium sensors it does not seem to be feasible to confirm a redox change before the first calcium spike. A recent study indicated that superoxide anion produced by X+XO in the extracellular space traverses the plasma membrane (34), providing a mechanism underlying the cytoplasmic $O_2^{\cdot-}$ rise and redox change.

Collectively, these data suggest that extracellular $O_2^{\cdot-}$ generation causes an intracellular $O_2^{\cdot-}$ increase and a dose-dependent activation of a $[Ca^{2+}]_c$ signalling pathway. Previously, we have also reported that exposure to X+XO causes mitochondrial membrane permeabilization and apoptosis but these effects only occurred after much longer exposures (1 hr or longer) (32).

**The $O_2^{\cdot-}$-induced $[Ca^{2+}]_c$ signal depends on $Ca^{2+}$ mobilization from the ER**

To clarify the source of the $[Ca^{2+}]_c$ signal, the $O_2^{\cdot-}$-generating system was first added to cells pretreated with thapsigargin (Tg, 2 μM) that discharges the ER $Ca^{2+}$ store. Tg pretreatment abolished the $O_2^{\cdot-}$-induced $[Ca^{2+}]_c$ signal (Fig3B vs 3A). By contrast, pretreatment of the cells with a mitochondrial uncoupler to eliminate the mitochondrial $Ca^{2+}$ storage (Fig3CE) or removal of extracellular $Ca^{2+}$ to prevent $Ca^{2+}$ entry (Fig3DE) failed to eliminate the $O_2^{\cdot-}$-induced $[Ca^{2+}]_c$ rise. Thus, the $O_2^{\cdot-}$-induced $[Ca^{2+}]_c$ signal is mediated by $Ca^{2+}$ mobilization from the ER and does not require $Ca^{2+}$ entry or mitochondrial $Ca^{2+}$ accumulation. Furthermore, the rapid kinetic of the $[Ca^{2+}]_c$ rise indicates the involvement of IP3Rs in the ER $Ca^{2+}$ mobilization.

**$O_2^{\cdot-}$-induced $[Ca^{2+}]_c$ signals in RBL-2H3 and DT40 cells**

To test if the $O_2^{\cdot-}$-induced $[Ca^{2+}]_c$ signal is cell type or species specific we also tested the effect of X+XO on the $[Ca^{2+}]_c$ in RBL-2H3 rat mast cells and in DT40 chicken B lymphocytes (Fig4). These cells were also selected because RBL-2H3 cells provide a model for the quantification of both $[Ca^{2+}]_c$ and $[Ca^{2+}]_m$ changes elicited by $IP_3$ addition (see Fig5) and DT40 cell clones expressing individual IP3R isoforms are available (Fig6-10). Similar to HepG2 cells, both RBL-2H3 and DT40 cells exhibited a $[Ca^{2+}]_c$ spike in response to $O_2^{\cdot-}$ generation (Fig4AB). In the RBL-2H3 cells, the $[Ca^{2+}]_c$ spike was regularly followed by baseline-spike $[Ca^{2+}]_c$ oscillations (Fig4A), whereas in the DT40 cells the $[Ca^{2+}]_c$ showed a plateau slightly above the baseline (Fig4B). These results indicate that $O_2^{\cdot-}$ induces rapid $Ca^{2+}$ mobilization in a variety of cell types regardless of the species of origin.

**$O_2^{\cdot-}$ promotes $IP_3$-induced $Ca^{2+}$ mobilization and mitochondrial $Ca^{2+}$ transfer in permeabilized RBL-2H3 cells**

A previous study has shown X+XO stimulating phospholipase-mediated $IP_3$ formation, which might lead to IP3R activation (35). To determine if $O_2^{\cdot-}$ has any effects downstream of $IP_3$ formation, we used permeabilized RBL-2H3 cells in which $Ca^{2+}$ mobilization can be directly activated by added $IP_3$. Also, in this model, a fraction of the IP3R-mediated $Ca^{2+}$ release is locally transferred to the mitochondria, which can be monitored simultaneously with the $Ca^{2+}$ release (22). When a suboptimal dose of $IP_3$ was added, the IP3R-mediated $Ca^{2+}$ release was greatly enhanced by $O_2^{\cdot-}$ (Fig5A, B lower). However, saturating $IP_3$ doses evoked comparable $[Ca^{2+}]_c$ increases in the absence and presence of $O_2^{\cdot-}$-generating system (Fig5B lower). $[Ca^{2+}]_m$ recorded simultaneously with $[Ca^{2+}]_c$ also showed great enhancement of the effect of suboptimal $IP_3$ and no change in the effect of maximal $IP_3$ (Fig5AB upper). The enhancement of the suboptimal $IP_3$-induced $[Ca^{2+}]_m$ signal appeared to be even more robust (~3-fold) than the increase in the $[Ca^{2+}]_c$ signal (~2-fold). These results suggest that $O_2^{\cdot-}$ sensitizes the IP3R-mediated $Ca^{2+}$ release, clarifying that the $O_2^{\cdot-}$-induced $[Ca^{2+}]_c$ signal in intact cells did not necessarily result from stimulation of $IP_3$ production. Furthermore, sensitization of the IP3R leads to a relatively large increase in the IP3R-mitochondrial $Ca^{2+}$ transfer, illustrating a striking consequence of the $O_2^{\cdot-}$ effect on local calcium signaling. The disproportionally large mitochondrial response might be evoked

because the local $Ca^{2+}$ transfer is more effective when IP3Rs are activated in a synchronous manner (22).

**Lack of IP3R1 and IP3R2 prevents the $O_2^{\cdot-}$-induced $[Ca^{2+}]_c$ signals in DT40 cells**

The studies described above have indicated that $O_2^{\cdot-}$ promotes IP3R activation by $IP_3$. Since the IP3R has 3 isoforms that display 60-70% homology in sequence and similarities in their regulation we wanted to clarify if every isoform can respond to $O_2^{\cdot-}$. For this purpose we used DT40 cells lacking various combinations of the IP3Rs (Fig6). In IP3R triple knockout (TKO) cells the $O_2^{\cdot-}$-induced $[Ca^{2+}]_c$ rise was absent (Fig6AB, second from left), confirming the dependence of the $O_2^{\cdot-}$-induced $Ca^{2+}$ mobilization on the presence of IP3Rs. DT40 cells lacking two out of three IP3R isoforms (DKO) expressing either type 1 (DKO1) or type 2 IP3Rs (DKO2) showed a $[Ca^{2+}]_c$ signal, whereas DKO expressing type 3 IP3R (DKO3) did not display any $[Ca^{2+}]_c$ elevation (Fig6AB). However, upon stimulation with IgM, an agonist that stimulates $IP_3$ formation every DKO but the TKO cells showed a $[Ca^{2+}]_c$ rise (Fig6C). Thus, every chicken IP3R isoform responds to $IP_3$ generation by mediating $[Ca^{2+}]_c$ oscillations but only IP3R1 and IP3R2 are sensitive to stimulation by $O_2^{\cdot-}$.

**Resistance of IP3R3 to $O_2^{\cdot-}$-induced sensitization in DT40 cells**

Next, we set out to test whether $O_2^{\cdot-}$ differentially sensitizes the various IP3R isoforms to $IP_3$ in permeabilized DT40 cells. First, the effect of $IP_3$ on the $Ca^{2+}$ storage pools was tested in cells expressing different IP3Rs. In wild type cells as well in every DKO, $IP_3$-induced a dose dependent $[Ca^{2+}]_c$ increase (Fig7A). Although, the size of the Tg-induced $[Ca^{2+}]_c$ increase was similar in each DT40 lines, including the TKO cells (Fig7C), the $IP_3$-sensitive increase was considerably smaller in the DKO3 cells than in the wild type or DKO1 and DKO2 cells (Fig7B). Furthermore, the $IP_3$ dose-response relationship was rightward shifted for the DKO3 cells, whereas the curves for DKO1 and DKO2 were very close to that for the wild type (Fig7D).

In wild type DT40 cells, the $O_2^{\cdot-}$ generating system promoted the $[Ca^{2+}]_c$ rise induced by a suboptimal $IP_3$ dose and failed to alter the effect of maximal $IP_3$ (Fig8A). Furthermore, DTT, a thiol protecting agent, slightly attenuated the $[Ca^{2+}]_c$ rise evoked by suboptimal $IP_3$ but did not change the response to maximal $IP_3$ (Fig8A). Thus, thiol oxidation controlled $IP_3$ sensitivity in DT40 cells expressing 3 IP3R isoforms. DTT-induced desensitization was also observed in DKO2, whereas the desensitization was not significant in DKO1 (Fig8B). Furthermore, the $IP_3$-sensitvity of DKO3 was not affected by $O_2^{\cdot-}$ or DTT (Fig8B). These results suggest that differential sensitization of IP3R1, IP3R2 and IP3R3 by $O_2^{\cdot-}$ might cause the different $[Ca^{2+}]_c$ signals in DKO1, DKO2 and DKO3.

**Sensitization of rat IP3R3 by $O_2^{\cdot-}$ in IP3R-triple knockout DT40 cells**

The relatively small size of the $IP_3$ releasable $Ca^{2+}$ storage and $IP_3$ sensitivity in DKO3 indicated that the IP3R expression level might be low. To test the dependency of the $Ca^{2+}$ pool size, $IP_3$ sensitivity and redox regulation on IP3R expression level, we used TKO cells rescued by IP3R3. Since full length chicken IP3R has not been cloned, the experiments were carried out in rat IP3R3 expressing stable TKO clones (Fig9). First, quantification of IP3R3 western blots of cell lysates was used to select 4 clones that showed a 10-fold range in IP3R3 expression level (100, 30, 17 and 12 %, normalized to the highest expressing clone). The highest $IP_3$ sensitivity was indeed associated with the highest IP3R3 expression and the $IP_3$ releasable fraction of the ER $Ca^{2+}$ store was consistently higher in every rat IP3R3 expressing clones than in the DKO3 (Fig9AB). Strikingly, every rat IP3R3 expressing TKO showed an apparent sensitization in the presence of $O_2^{\cdot-}$ generating system (Fig9C). Collectively, these results indicate that $O_2^{\cdot-}$ sensitizes IP3R regardless of their expression level. Surprisingly, the rat IP3R3 is similar to chicken IP3R1 and IP3R2 in its sensitivity to $O_2^{\cdot-}$.

**Sequence heterogeneity between chicken IP3R3 and other IP3R isoforms**

$O_2^{\cdot-}$ likely affects the IP3R function through a reactive Cys residue(s) within the IP3R or in a protein that interacts with and controls the IP3R. Since the latter group includes many proteins, we focused on studying the presence of Cys thiol groups in various IP3R isoforms. We searched for a Cys that is present it rat but is absent in chicken IP3R3. We found that 3 out of 51 Cys-s present in rat IP3R3 were absent in

chicken IP3R3 (Table1). However, none of these Cys-s was also present in IP3R1 and IP3R2. Thus, these Cys groups are unlikely to confer $O_2^{\cdot-}$ sensitivity to the IP3R.

In order to determine if there are differences in the redox responses of the chicken and rat IP3R3s, we measured the redox state of the receptors expressed in DT40 cells using a modification of the thiol trapping procedure described in (25) (Fig10). In this method, TCA is used to deproteinize the cells and prevent thiol transformations. The precipitated protein is solubilized under denaturing conditions (SDS/Urea) and successively treated with iodoacetamide and DTT to block free thiol groups and to make available oxidized residues for subsequent reaction with maleimide conjugated to a 5 kDa polyethyleneglycol (MPEG-5). The magnitude of the gel shift in immunoreactive IP3R is proportional to the number of available oxidized residues in the protein. The minimal shift observed for the chicken and rat IP3R3 is an indication that very few of the thiol residues in the receptor are oxidized under control conditions. The addition of X+XO to the cells expressing the rat IP3R3 isoform resulted in an enhanced reactivity of the receptor for MPEG-5 indicating the oxidation of additional thiols. By contrast the chicken isoform did not show an enhanced MPEG-5 shift. A similar difference was also noted in response to 0.2 mM $H_2O_2$ (data not shown). Thus, some evolutionary conserved Cys are likely to be modified by $O_2^{\cdot-}$ only in the rat IP3R3 and are candidates to mediate sensitization of the IP3R to IP3.

**Discussion**

Our studies demonstrate $O_2^{\cdot-}$-dependent sensitization of $IP_3$-induced $Ca^{2+}$ release towards $IP_3$, which is likely to contribute to $O_2^{\cdot-}$-induced $[Ca^{2+}]_c$ spikes and oscillations. Furthermore, the $O_2^{\cdot-}$-induced sensitization appears as a particularly potent facilitator of the ER-mitochondrial $Ca^{2+}$ transfer presumably, due to its dependence on synchronized activation of IP3Rs, which is effectively supported by $O_2^{\cdot-}$. This work also provides evidence that the IP3R sensitization by $O_2^{\cdot-}$ is IP3R isoform and species specific. $O_2^{\cdot-}$ fails to induce sensitization of the chicken IP3R3. The differential effect of $O_2^{\cdot-}$ on chicken IP3R3 and chicken IP3R1 and 2 or rat IP3R3 is likely to be mediated by a conserved cysteine residue(s) that is less reactive in the chicken IP3R3. Overall, this study provides the first evidence that physiologically relevant ROS can control cytoplasmic and mitochondrial calcium signaling through the IP3Rs.

The sensitization of IP3Rs by exogenous oxidants is well established in the literature but the molecular mechanisms involved have not been elucidated (reviewed in (11)). Most recently, Khan et al (36) have examined the effect of thimerosal on the IP3 responses of permeabilized DT40 cells expressing various rat IP3R isoforms. They showed that the types IP3R1 and IP3R2 were sensitized by thimerosal but that the rat IP3R3 was not. In our study, the rat IP3R3 expressed in DT40 cells retained responsiveness to a physiologically relevant oxidant, $O_2^{\cdot-}$. Apart from differences in the oxidants employed, the basis for this discrepancy is presently unclear. However, our results demonstrated that $O_2^{\cdot-}$ causes modification of a thiol-group of the rat IP3R3, which might mediate the sensitization. Based on sequence analysis, the $O_2^{\cdot-}$-sensitive site is also present in the chicken IP3R3 but based on the "thiol trapping" studies, is unaccessible for modification. As to the nature of the oxidative modifications, several possibilities are available, including disulphide bridge formation and S-glutathionylation. Disulphide bridge formation has been described only at the ER luminal domain of the IP3R (37) which is unlikely in the present case due to the low membrane permeability of $O_2^{\cdot-}$. Although $O_2^{\cdot-}$ could be converted to $H_2O_2$ that is also a prooxidant and can traverse the ER membrane, the resting $[H_2O_2]$ is already very high in the ER lumen (38). S-glutathionylation of the IP3R1 has been demonstrated during diamide sensitization of the IP3R in cultured aortic endothelial cells (16,17). Whether this is a general modification occurring with other oxidants, IP3R isoforms and cell types remains to be determined.

Redox regulation of ryanodine receptors (RyRs) channels share several common features with IP3Rs. RyRs show enhanced activity in response to exogenous oxidants as well as endogenously produced ROS in both heart and skeletal muscle (39,40). Attempts to identify the redox sensitive, "hyper-reactive" thiols by mass spectrometry indicate the involvement of multiple thiols dispersed throughout the linear sequence

(41,42). Mutagenesis of multiple residues did not entirely eliminate the functional effects of the redox agents (43). In addition the findings in the present paper indicate that redox sensitivity may not solely be determined by thiols on the IP3R, but could also involve other factors, such as associated proteins or the local environment. This suggests that unraveling the molecular basis of redox sensing in these intracellular $Ca^{2+}$ release channels will be a challenging task.

Recent studies indicate broad physiological and pathophysiological relevance of ROS (44,45). The present results suggest that $O_2^{\cdot-}$ produced by multiple intracellular enzymes might utilize IP3R-mediated $Ca^{2+}$ mobilization to make a contribution to cell signaling. Since DTT that reduces disulphide bonds in proteins had some desensitizing effects on the IP3R activity under resting conditions, low levels of ROS continually produced inside the cells, might be relevant for IP3R function. However, the large effect of the $O_2^{\cdot-}$ generating system indicates that increased endogenous ROS production has the potential to enhance IP3R-linked calcium signaling. Our studies primarily focused on the effects of $O_2^{\cdot-}$ however, its breakdown product, $H_2O_2$ also seems to have sensitizing effect on the IP3R ((46,47) and present results). ROS can also be converted to reactive nitrogen species (RNS), and RNS-mediated nitrosylation affects some components of calcium signaling but its relevance for the IP3R is unclear.

Production of $O_2^{\cdot-}$ elicited frequency-modulated baseline-spike $[Ca^{2+}]_c$ oscillation phenotype. While some models of $[Ca^{2+}]_c$ oscillations depend on fluctuations in $[IP_3]$ (48), we have also shown that exposure of IP3R to a stable $[IP_3]$ is sufficient to elicit $[Ca^{2+}]_c$ oscillations mediated by positive and negative feedback effects of $Ca^{2+}$ on IP3Rs (49). Thus, $O_2^{\cdot-}$ induced sensitization of the IP3R to $IP_3$ might be able to promote $[Ca^{2+}]_c$ oscillations at relatively low and stable $[IP_3]$. Notably, our results support that extracellular superoxide anion increases cytoplasmic ROS, which can directly control $IP_3$-induced $Ca^{2+}$ release. It remains possible that a component of the calcium signaling response observed in intact cells is also due to enhanced $IP_3$ formation which could also be secondary to elevated $[Ca^{2+}]_c$.

The IP3Rs represent an intriguing target of ROS owing to their localization close to main ROS producing organelles (50). Both the ER that hosts IP3Rs and the mitochondria that are closely associated and physically coupled to the ER are central to cellular ROS production. It has been speculated that ROS produced by these organelles can locally expose the IP3Rs and RyRs (50,51). However, these ideas remain to be tested by direct measurements of ROS at cellular subdomains. Our demonstration of the potential functional relevance of ROS in both ER $Ca^{2+}$ mobilization and local $Ca^{2+}$ transfer to the mitochondria should stimulate further studies of ROS at the surface and interface of ER and mitochondria.

**Acknowledgements**

We thank Dr. T. Kurosaki for providing us with DT40 cells. Száva Bánsághi was generously supported by an HAESF International Research Fellowship**.** This study was funded by NIH grants to G.H. (GM059419), S.K.J. (DK34804) and K.S. (DK053867).

## References

1. Berridge, M. J. (2009) Inositol trisphosphate and calcium signalling mechanisms. *Biochim.Biophys Acta* **1793**, 933-940
2. Mikoshiba, K. (2007) IP3 receptor/Ca2+ channel: from discovery to new signaling concepts. *J Neurochem.* **102**, 1426-1446
3. Petersen, O. H., and Tepikin, A. V. (2008) Polarized calcium signaling in exocrine gland cells. *Annu.Rev.Physiol* **70**, 273-299
4. Sanderson, M. J., Delmotte, P., Bai, Y., and Perez-Zogbhi, J. F. (2008) Regulation of airway smooth muscle cell contractility by Ca2+ signaling and sensitivity. *Proc.Am.Thorac.Soc.* **5**, 23-31

5. Lewis, R. S. (2001) Calcium signaling mechanisms in T lymphocytes. *Annu.Rev.Immunol.* **19**, 497-521
6. Malcuit, C., Kurokawa, M., and Fissore, R. A. (2006) Calcium oscillations and mammalian egg activation. *J Cell Physiol* **206**, 565-573
7. Szalai, G., Krishnamurthy, R., and Hajnoczky, G. (1999) Apoptosis driven by IP(3)-linked mitochondrial calcium signals. *The EMBO journal* **18**, 6349-6361
8. Vanderheyden, V., Devogelaere, B., Missiaen, L., De Smedt, H., Bultynck, G., and Parys, J. B. (2009) Regulation of inositol 1,4,5-trisphosphate-induced Ca2+ release by reversible phosphorylation and dephosphorylation. *Biochim.Biophys Acta* **1793**, 959-970
9. Betzenhauser, M. J., and Yule, D. I. (2010) Regulation of inositol 1,4,5-trisphosphate receptors by phosphorylation and adenine nucleotides. *Curr.Top.Membr.* **66C**, 273-298
10. Patterson, R. L., Boehning, D., and Snyder, S. H. (2004) Inositol 1,4,5-trisphosphate receptors as signal integrators. *Annual review of biochemistry* **73**, 437-465
11. Joseph, S. K. (2010) Role of thiols in the structure and function of IP3 receptors. *Current Topics Membrane transport* **66**, 299-322
12. Bootman, M. D., Taylor, C. W., and Berridge, M. J. (1992) The thiol reagent, thimerosal, evokes Ca2+ spikes in HeLa cells by sensitizing the inositol 1,4,5-trisphosphate receptor. *J Biol.Chem.* **267**, 25113-25119
13. Bultynck, G., Szlufcik, K., Kasri, N. N., Assefa, Z., Callewaert, G., Missiaen, L., Parys, J. B., and De Smedt, H. (2004) Thimerosal stimulates Ca2+ flux through inositol 1,4,5-trisphosphate receptor type 1, but not type 3, via modulation of an isoform-specific Ca2+-dependent intramolecular interaction. *Biochem.J.* **381**, 87-96
14. Khan, S. A., Rossi, A. M., Riley, A. M., Potter, B. V., and Taylor, C. W. (2013) Subtype-selective regulation of IP(3) receptors by thimerosal via cysteine residues within the IP(3)-binding core and suppressor domain. *The Biochemical journal* **451**, 177-184
15. Bird, G., Burgess, G., and Putney, J. W., Jr. (1993) Sulfhydryl reagents and cAMP-dependent kinase increase the sensitivity of the inositol 1,4,5-trisphosphate receptor in hepatocytes. *J.Biol.Chem.* **268**, 17917-17923
16. Lock, J. T., Sinkins, W. G., and Schilling, W. P. (2011) Effect of protein S-glutathionylation on Ca2+ homeostasis in cultured aortic endothelial cells. *Am.J Physiol Heart Circ.Physiol* **300**, H493-H506
17. Lock, J. T., Sinkins, W. G., and Schilling, W. P. (2012) Protein S-glutathionylation enhances Ca2+-induced Ca2+ release via the IP3 receptor in cultured aortic endothelial cells. *The Journal of physiology* **590**, 3431-3447
18. Joseph, S. K., Lin, C., Pierson, S., Thomas, A. P., and Maranto, A. R. (1995) Heteroligomers of type-I and type-III Inositol Trisphosphate receptors in WB rat liver epithelial cells. *J.Biol.Chem.* **270**, 23310-23316
19. Wojcikiewicz, R. J., and He, Y. (1995) Type I, II and III Inositol 1,4,5-Trisphosphate receptor co-immunoprecipitation as evidence for the existence heterotetrameric receptor complexes. *Biochem.Biophys.Res.Commun.* **213**, 334-341
20. Mendes, C. C., Gomes, D. A., Thompson, M., Souto, N. C., Goes, T. S., Goes, A. M., Rodrigues, M. A., Gomez, M. V., Nathanson, M. H., and Leite, M. F. (2005) The type III inositol 1,4,5-trisphosphate receptor preferentially transmits apoptotic Ca2+ signals into mitochondria. *The Journal of biological chemistry*
21. Brown, G. C., and Borutaite, V. (2012) There is no evidence that mitochondria are the main source of reactive oxygen species in mammalian cells. *Mitochondrion.* **12**, 1-4

22. Csordas, G., Thomas, A. P., and Hajnoczky, G. (1999) Quasi-synaptic calcium signal transmission between endoplasmic reticulum and mitochondria. *The EMBO journal* **18**, 96-108
23. Csordas, G., Renken, C., Varnai, P., Walter, L., Weaver, D., Buttle, K. F., Balla, T., Mannella, C. A., and Hajnoczky, G. (2006) Structural and functional features and significance of the physical linkage between ER and mitochondria. *The Journal of cell biology* **174**, 915-921
24. Betzenhauser, M. J., Wagner, L. E., 2nd, Won, J. H., and Yule, D. I. (2008) Studying isoform-specific inositol 1,4,5-trisphosphate receptor function and regulation. *Methods* **46**, 177-182
25. Leichert, L. I., and Jakob, U. (2004) Protein thiol modifications visualized in vivo. *PLoS biology* **2**, e333
26. Csordas, G., and Hajnoczky, G. (2001) Sorting of calcium signals at the junctions of endoplasmic reticulum and mitochondria. *Cell calcium* **29**, 249-262
27. Pacher, P., Sharma, K., Csordas, G., Zhu, Y., and Hajnoczky, G. (2008) Uncoupling of ER-mitochondrial calcium communication by transforming growth factor-beta. *American journal of physiology. Renal physiology* **295**, F1303-1312
28. Akerboom, J., Carreras Calderon, N., Tian, L., Wabnig, S., Prigge, M., Tolo, J., Gordus, A., Orger, M. B., Severi, K. E., Macklin, J. J., Patel, R., Pulver, S. R., Wardill, T. J., Fischer, E., Schuler, C., Chen, T. W., Sarkisyan, K. S., Marvin, J. S., Bargmann, C. I., Kim, D. S., Kugler, S., Lagnado, L., Hegemann, P., Gottschalk, A., Schreiter, E. R., and Looger, L. L. (2013) Genetically encoded calcium indicators for multi-color neural activity imaging and combination with optogenetics. *Frontiers in molecular neuroscience* **6**, 2
29. Meyer, A. J., and Dick, T. P. (2010) Fluorescent protein-based redox probes. *Antioxidants & redox signaling* **13**, 621-650
30. Gutscher, M., Pauleau, A. L., Marty, L., Brach, T., Wabnitz, G. H., Samstag, Y., Meyer, A. J., and Dick, T. P. (2008) Real-time imaging of the intracellular glutathione redox potential. *Nature methods* **5**, 553-559
31. Csordas, G., Golenar, T., Seifert, E. L., Kamer, K. J., Sancak, Y., Perocchi, F., Moffat, C., Weaver, D., de la Fuente Perez, S., Bogorad, R., Koteliansky, V., Adijanto, J., Mootha, V. K., and Hajnoczky, G. (2013) MICU1 controls both the threshold and cooperative activation of the mitochondrial Ca(2)(+) uniporter. *Cell metabolism* **17**, 976-987
32. Madesh, M., and Hajnoczky, G. (2001) VDAC-dependent permeabilization of the outer mitochondrial membrane by superoxide induces rapid and massive cytochrome c release. *The Journal of cell biology* **155**, 1003-1015
33. Dooley, C. T., Dore, T. M., Hanson, G. T., Jackson, W. C., Remington, S. J., and Tsien, R. Y. (2004) Imaging dynamic redox changes in mammalian cells with green fluorescent protein indicators. *The Journal of biological chemistry* **279**, 22284-22293
34. Hawkins, B. J., Madesh, M., Kirkpatrick, C. J., and Fisher, A. B. (2007) Superoxide flux in endothelial cells via the chloride channel-3 mediates intracellular signaling. *Molecular biology of the cell* **18**, 2002-2012
35. Madesh, M., Hawkins, B. J., Milovanova, T., Bhanumathy, C. D., Joseph, S. K., Ramachandrarao, S. P., Sharma, K., Kurosaki, T., and Fisher, A. B. (2005) Selective role

for superoxide in InsP3 receptor-mediated mitochondrial dysfunction and endothelial apoptosis. *The Journal of cell biology* **170**, 1079-1090

36. Khan, S. A., Rossi, A. M., Riley, A. M., Potter, B. V., and Taylor, C. W. (2013) Subtype-selective regulation of IP3 receptors by thimerosal via cysteine residues within the IP3-binding core and suppressor domain. *Biochem.J*
37. Higo, T., Hattori, M., Nakamura, T., Natsume, T., Michikawa, T., and Mikoshiba, K. (2005) Subtype-specific and ER lumenal environment-dependent regulation of inositol 1,4,5-trisphosphate receptor type 1 by ERp44. *Cell* **120**, 85-98
38. Enyedi, B., Varnai, P., and Geiszt, M. (2010) Redox state of the endoplasmic reticulum is controlled by Ero1L-alpha and intraluminal calcium. *Antioxidants & redox signaling* **13**, 721-729
39. Donoso, P., Sanchez, G., Bull, R., and Hidalgo, C. (2011) Modulation of cardiac ryanodine receptor activity by ROS and RNS. *Front Biosci.* **16**, 553-567
40. Prosser, B. L., Khairallah, R. J., Ziman, A. P., Ward, C. W., and Lederer, W. J. (2012) X-ROS signaling in the heart and skeletal muscle: Stretch-dependent local ROS regulates [Ca(2+)](i). *J Mol.Cell Cardiol.* **58**, 172-181
41. Voss, A. A., Lango, J., Ernst-Russell, M., Morin, D., and Pessah, I. N. (2004) Identification of hyperreactive cysteines within ryanodine receptor type 1 by mass spectrometry. *The Journal of biological chemistry* **279**, 34514-34520
42. Aracena-Parks, P., Goonasekera, S. A., Gilman, C. P., Dirksen, R. T., Hidalgo, C., and Hamilton, S. L. (2006) Identification of cysteines involved in S-nitrosylation, S-glutathionylation, and oxidation to disulfides in ryanodine receptor type 1. *J Biol.Chem.* **281**, 40354-40368
43. Petrotchenko, E. V., Yamaguchi, N., Pasek, D. A., Borchers, C. H., and Meissner, G. (2011) Mass spectrometric analysis and mutagenesis predict involvement of multiple cysteines in redox regulation of the skeletal muscle ryanodine receptor ion channel complex. *Res.Rep.Biol* **2011**, 13-21
44. Sena, L. A., and Chandel, N. S. (2012) Physiological roles of mitochondrial reactive oxygen species. *Molecular cell* **48**, 158-167
45. Malhotra, J. D., and Kaufman, R. J. (2007) Endoplasmic reticulum stress and oxidative stress: a vicious cycle or a double-edged sword? *Antioxidants & redox signaling* **9**, 2277-2293
46. Redondo, P. C., Salido, G. M., Rosado, J. A., and Pariente, J. A. (2004) Effect of hydrogen peroxide on Ca2+ mobilisation in human platelets through sulphydryl oxidation dependent and independent mechanisms. *Biochemical pharmacology* **67**, 491-502
47. Zheng, Y., and Shen, X. (2005) H2O2 directly activates inositol 1,4,5-trisphosphate receptors in endothelial cells. *Redox report : communications in free radical research* **10**, 29-36
48. Thomas, A. P., Bird, G. S., Hajnoczky, G., Robb-Gaspers, L. D., and Putney, J. W., Jr. (1996) Spatial and temporal aspects of cellular calcium signaling. *FASEB journal : official publication of the Federation of American Societies for Experimental Biology* **10**, 1505-1517
49. Hajnoczky, G., and Thomas, A. P. (1997) Minimal requirements for calcium oscillations driven by the IP3 receptor. *The EMBO journal* **16**, 3533-3543
50. Csordas, G., and Hajnoczky, G. (2009) SR/ER-mitochondrial local communication: calcium and ROS. *Biochimica et biophysica acta* **1787**, 1352-1362

51. Brookes, P. S., Yoon, Y., Robotham, J. L., Anders, M. W., and Sheu, S. S. (2004) Calcium, ATP, and ROS: a mitochondrial love-hate triangle. *American journal of physiology. Cell physiology* **287**, C817-833

## Figure Legends

**Fig 1: Generation of $O_2^{\cdot-}$ causes dose-dependent $[Ca^{2+}]_c$ oscillations in HepG2 cells**

**A** $[Ca^{2+}]_c$ was measured in fura2/AM-loaded intact HepG2 cells treated with xanthine (X) 100 μM +xanthine oxidase (XO) 20 mU/ml to produce $O_2^{\cdot-}$. In the images recorded before (40s) and after X+XO addition (70s), the green to red shift (F 340nm/F380nm increase) indicates a $[Ca^{2+}]_c$ elevation in most cells. For the cells, marked by the numbers on them the time course shows that $[Ca^{2+}]_c$ spikes and baseline spike oscillations were elicited by X+XO (graphs).

**B** Individual and mean cell $[Ca^{2+}]_c$ time course records obtained during exposure to different doses of XO (20, 5 and 1 mU/ml). Mean was calculated for all cells (responding and non-responding) in the field.

**C-E** X+XO dose-dependence of the lag time (C), fraction of responding cells (D) and magnitude of the $[Ca^{2+}]_c$ rise (E).

Data in E also shows that heat-inactivated XO (10min incubation in boiling water) fails to cause a $[Ca^{2+}]_c$ rise.

**Fig 2: Extracellular generation of $O_2^{\cdot-}$ causes a rapid and dynamic response in the cytoplasmic redox state**

**A** $[Ca^{2+}]_c$ and glutathione redox state were measured simultaneously in RCaMP and Grx1-roGFP2-expressing intact HepG2 cells treated with xanthine (X) 100 μM +xanthine oxidase (XO) 20 mU/ml to produce $O_2^{\cdot-}$. The time course shows the $[Ca^{2+}]_c$ spikes recorded in the individual cells of the imaging field (red) and the mean response in the GSH redox state (black). The mean response faithfully represents the kinetic of the single cell responses that were averaged because of the relatively low signal to noise ratio.

B Single cell Grx1-roGFP2 ratios obtained at 1min of stimulation were normalized to the prestimulation ratio values (90s before stimulation) and the mean was calculated for cells treated with X+XO and with X alone, respectively (9 measurements for each, ~10 cells/measurement). A significant increase was obtained for X+XO as compared to X alone ($p<0.03$). Please note that a continuous downward baseline drift caused lowering $R_{160s}/R_{10s}$ under 1 in 150s.

**Fig 3: The $O_2^{\cdot-}$-induced $[Ca^{2+}]_c$ signal requires ER $Ca^{2+}$-mobilization but is not dependent on $Ca^{2+}$ entry or mitochondrial $Ca^{2+}$ storage**

**A-D** Mean $[Ca^{2+}]_c$ time course is shown for all cells (10-20cells) in the imaging field:

**A** X+XO 20 mU/ml-induced $[Ca^{2+}]_c$ rise.

**B** ER $Ca^{2+}$ store predepletion with Tg (2 μM) treatment prevented the $O_2^{\cdot-}$–induced $[Ca^{2+}]_c$ rise.

**C** Uncoupling of the mitochondria by FCCP (5 μM)+oligomycin (5 μg/ml) pretreatment did not interfere with the $O_2^{\cdot-}$–induced $[Ca^{2+}]_c$ rise.

**D** Incubation of the cells in a nominally $Ca^{2+}$ free medium did not prevent the $O_2^{\cdot-}$ induced $[Ca^{2+}]_c$ rise.

**E** Bar charts show the summary of the individual cell records shown in A-D (n=50-100 cells)

**Fig 4: $O_2^{\cdot-}$ evokes a $[Ca^{2+}]_c$ signal in a variety of cell types**

X+XO (20 mU/ml)-induced $[Ca^{2+}]_c$ signal in intact **A** RBL-2H3 and **B** DT40 cells loaded with fura2/AM. The upper graphs shows the mean $[Ca^{2+}]_c$ rise, whereas the other graphs illustrate the heterogeneity of the individual cell responses.

**Fig 5: $O_2^{\cdot-}$ promotes $IP_3$-induced $Ca^{2+}$ mobilization and mitochondrial $Ca^{2+}$ transfer in permeabilized cells**

Mitochondrial and cytosolic [$Ca^{2+}$] were measured simultaneously in suspensions of permeabilized RBL-2H3 cells, which were either untreated (control) or pretreated with X + XO. Responses were measured by furaFF/AM compartmentalized in the mitochondria (upper graphs) and by rhod2/FA in the cytosol (lower graphs). A) Time courses of responses to suboptimal IP3 (50 nM). B) Mean responses to suboptimal IP3 (50 nM) and maximal IP3 (7.5 μM) (n=4-5).

**Fig 6: IP3R isoform dependent $O_2^{\cdot-}$-induced $[Ca^{2+}]_c$ signal in intact DT40 cells**

**A** Time course of the X+XO (20 mU/ml)-induced $[Ca^{2+}]_c$ signal is shown in wild type (WT), IP3R triple knockout (TKO) and double knockout (DKO) individual DT40 cells. The $O_2^{\cdot-}$-induced $[Ca^{2+}]_c$ signal was absent in TKO cells. Similarly, IP3R3 expressing DT40 cells also failed to respond to $O_2^{\cdot-}$, whereas only IP3R1 (DKO1) and IP3R2 (DKO2) expressing cells showed a $[Ca^{2+}]_c$ signal.

**B** Summary of the peak $[Ca^{2+}]_c$ increases obtained in the 5 different cell types.

**C** Time course of the $[Ca^{2+}]_c$ signal evoked by IgM (2 μg/ml), a phospholipase C-coupled agonist in each DT40 cell type. Every DKO cell type expressing at least one IP3R isoform, even IP3R3, showed an IgM-induced $[Ca^{2+}]_c$ signal.

**Fig 7: $IP_3$ sensitivity of the ER $Ca^{2+}$ storage pools in DT40 cells expressing various IP3R isoforms**

$IP_3$-induced $Ca^{2+}$ mobilization was measured in suspensions of permeabilized DT40 cells.

**A** $[Ca^{2+}]_c$ increases evoked by sequential additions of suboptimal (100 nM), maximal (7.5 μM) concentrations of $IP_3$, thapsigargin (Tg, 2 μM) and Ionomycin (Iono, 10 μM) are shown for DKO1, DKO2 and DKO3 cells.

**BC** Summary of the peak $[Ca^{2+}]_c$ increases evoked by $IP_3$ (7.5 μM, **B**) and Tg (2 μM, **C**) in wild type, TKO and DKO cells.

**D** $IP_3$ dose-response for $[Ca^{2+}]_c$ increases in wild type cells and various DKO cells (each symbol represents a separate measurement).

**Fig 8: $O_2^{\cdot-}$ sensitizes IP3R1 and IP3R2 to $IP_3$-induced $Ca^{2+}$ mobilization**

$IP_3$ induced $Ca^{2+}$ mobilization was measured in the presence or absence of X+XO (100 μM and 20 mU) or DTT (1 mM), a thiol protecting agent in suspensions of permeabilized cells using fura2/FA.

**A** The $[Ca^{2+}]_c$ increases evoked by both suboptimal (100 nM) and maximal (7.5 μM) concentrations of $IP_3$ are shown for WT DT40 cells (n=12). X+XO increased and DTT decreased the response to suboptimal $IP_3$ ($p< 0.03$) but did not alter significantly the effect of maximal $IP_3$. These results indicate $O_2^{\cdot-}$induced sensitization of the IP3Rs.

**B** $[Ca^{2+}]_c$ increases mediated be individual IP3R isoforms were monitored in DKO1 (n=11), DKO2 (n=15) and DKO3 (n=18) cells. Because of the different $IP_3$ sensitivity of IP3R1, IP3R2 and IP3R3, different suboptimal $IP_3$ concentrations were used for each cell type to attain approx. 30% $[Ca^{2+}]_c$ increase relative to the effect of the maximal $IP_3$. $O_2^{\cdot-}$ caused sensitization of IP3R1 and IP3R2 ($p< 0.01$) but failed to affect IP3R3.

**Fig 9: $O_2^{\cdot-}$ differently sensitizes chicken and rat IP3R3s**

The effect of X+XO on $[Ca^{2+}]_c$ increase was tested in suspensions of permeabilized DKO3 and in TKO rescued with rat IP3R3 (Clones expressing the most IP3R (100%), 30%, 17% and 12% are marked by yellow, red, green and blue colors, respectively).
**A** $IP_3$ dose-response relationships show that TKO cells expressing varying amounts of rat IP3R are more sensitive to $IP_3$ than the chicken IP3R3 expressing DKO3 cells.
**B Left.** Cumulative data for DKO3 and TKO cells expressing varying amounts of rat IP3R3. Cells were treated with the amount of $IP_3$ that mobilizes 30% of stored calcium as determined in A: 750 nM $IP_3$ for DKO3 cells and 400nM for TKO cells. Responses of TKO cells are relative to the response to 7.5 μM $IP_3$. **Right.** Cumulative responses to 7.5 μM $IP_3$ normalized to the total Tg-sensitive storage in each cell line.
**C** X+XO-induced sensitization in rat IP3R3 expressing cells. Rescue clones expressing rat IP3R3 at lower levels showed lesser $IP_3$ sensitivity but were also sensitized by $O_2^{\cdot-}$.

**Fig 10: $O_2^{\cdot-}$ induced thiol oxidation is absent in chicken IP3R3 but is present in rat IP3R3**
Trichloroacetic acid and a strongly denaturing buffer (SDS/Urea) was used to prepare lysates from control and X+XO treated DT40 cells expressing rat IP3R3 (TKO rescued with rat IP3R3) or chicken IP3R3 (DKO3) as described in "Materials and Methods". After initially blocking all free thiol groups with iodoacetamide, the remaining modified thiol residues were reduced with DTT and then reacted with MPEG-5. The presence of oxidized thiol residues in the receptor is indicated by a gel shift reaction detected by immunoblotting on 5% SDS PAGE. The data shown indicates that the thiols in the endogenous rat or chicken IP3R3 receptor are almost entirely in the reduced state under control conditions and only the rat isoform shows an oxidation response with X+XO. Because of differences in the expression levels of the chicken and rat isoforms the amount of protein loaded for the two isoforms was different (2 μg rat; 20 μg chicken). The data shown is representative of 3 experiments.

**Table1 Alignment of amino acid sequence of the different IP3Rs from various species**

To identify the relevant Cys thiol group in the $O_2^{\cdot-}$ -induced $[Ca^{2+}]_c$ signal we aligned the amino acid sequences of the 3 different IP3Rs from the various species. Analysis of the sequences indicates that 3 of the 51 cysteines present in the rat IP3R3 isoform are not conserved in the chicken or in the other 2 rat IP3R isoforms.

| **IP3R3** | | | | | | | 1558 | | | | | |
|---|---|---|---|---|---|---|---|---|---|---|---|---|
| Rat | L | S | S | G | G | S | C | S | A | A | A | Q |
| Mouse | L | S | S | G | G | S | C | S | A | A | A | Q |
| Human | L | S | S | G | A | S | C | A | A | A | A | Q |
| Chicken | L | N | S | - | - | S | S | T | S | T | V | Q |
| Zebrafish | L | S | S | - | - | S | N | S | L | T | L | S |
| **IP3R1** | | | | | | 1569 | | | | | | |
| Rat | F | L | K | S | H | N | - | - | - | I | V | Q |
| | | | | | | 1567 | | | | | | |
| Chicken | F | L | K | S | H | N | - | - | - | I | V | Q |
| **IP3R2** | | | | | 1576 | | | | | | | |
| Rat | F | M | K | N | H | - | - | S | S | T | V | Q |
| | | | | | | | 1569 | | | | | |
| Chicken | F | M | K | - | - | S | H | S | N | M | V | Q |

| **IP3R3** | | | | | 1738 | | | | |
|---|---|---|---|---|---|---|---|---|---|
| Rat | T | K | L | V | C | D | L | I | T |
| Mouse | T | K | L | V | C | D | L | I | T |
| Human | T | K | L | V | C | D | L | I | T |
| Chicken | T | K | L | V | A | D | L | I | M |
| Zebrafish | T | K | L | F | T | D | L | I | T |
| **IP3R1** | | | | | 1808 | | | | |
| Rat | S | N | L | V | I | D | L | I | M |
| | | | | | 1768 | | | | |
| Chicken | S | N | L | V | I | D | L | I | M |
| **IP3R2** | | | | | 1759 | | | | |
| Rat | S | E | L | V | I | D | V | I | V |
| | | | | | 1761 | | | | |
| Chicken | S | E | L | V | I | D | V | I | V |

| **IP3R3** | | | | | 2667 | | | C term |
|---|---|---|---|---|---|---|---|---|
| Rat | D | V | Q | N | C | M | S | R |
| Mouse | D | V | Q | N | C | M | S | R |
| Human | D | V | Q | N | C | I | S | R |
| Chicken | D | V | Q | N | T | M | N | H |
| Zebrafish | D | V | Q | S | G | S | N | P |
| **IP3R1** | | | | | | | | |
| Rat | - | - | - | - | - | - | - | - |
| Chicken | - | - | - | - | - | - | - | - |
| **IP3R2** | | | | | | | | |
| Rat | - | - | - | - | - | - | - | - |
| Chicken | - | - | - | - | - | - | - | - |